Solar Energy 230 (2021) 449–461

Contents lists available at ScienceDirect

Solar Energy

journal homepage: www.elsevier.com/locate/solener

Experimental investigation of the impact of urban fabric on canyon albedo using a 1:10 scaled physical model

Alkis Kotopouleas, Renganathan Giridharan, Marialena Nikolopoulou, Richard Watkins, Muhammed Yeninarcilar

Centre for Architecture and Sustainable Environment (CASE), Kent School of Architecture and Planning, University of Kent, Canterbury CT2 7NZ, United Kingdom

ARTICLE INFO

Keywords:
Urban fabric
Street canyon
Albedo
Façade materials
Reflectance
Infrared

ABSTRACT

This paper presents findings from a large-scale experiment on the impact of urban fabric on canyon albedo, aimed at informing the development of an urban albedo calculator for London, an empirical model to predict changes in urban albedo in relation to changes in urban fabric and solar altitude. Through different material applications on a 1:10 scaled physical model of an actual residential area, the study assessed the effect of street-level materials and three common façade types on canyon albedo alongside the canyon's reflective power in the infrared, and the impact of rain. The results showed that the addition of concrete paving at street level increased canyon albedo by 9%, while the substitution of tarmac with grass by 70%. Brickwork and aluminium cladding façades were seen to contribute to significantly higher canyon albedo than curtain wall across the measured irradiance spectrum. The results also revealed the highly dynamic nature of canyon albedo and a consistent rainfall-induced reduction of albedo in the range 22–36% throughout the experimental phases. The findings from this study can inform urban planning and policy making directed at tackling the urban heat island effect.

1. Introduction

Urban street canyons are fundamental elements of urban settings shaping our cities. Canyon albedo, the capacity of urban surfaces within a canyon to reflect solar radiation out of the canyon, is defined as the dimensionless fraction of reflected to incident radiation measured on a scale from 0 to 1. An albedo value of 0 indicates 100% absorption of the incident radiation and no reflective capability, as a perfectly black surface would demonstrate, while an albedo of 1 denotes 100% reflection of the incident radiation.

The albedo of street canyons is decisive for the reflective power of urban areas, i.e. urban albedo. The reduction of urban albedo is directly associated with the intensification of the urban heat island (UHI) phenomenon where temperatures in urban centres are higher than the surrounding rural areas. It is therefore an important determinant of changes in outdoor ambient temperature (Oke, 1988) and has implications for outdoor thermal comfort (Mishra & Ramgopal, 2013; Pantavou et al., 2011; Steemers et al., 1998) and building energy demand for cooling (Hassid et al., 2000; Kolokotroni et al., 2007). The apparent links to ambient temperature and human health have been recognised in several cities around the world (Hajat et al., 2010) where high temperatures have been correlated with increased rates of morbidity and mortality (Anderson & Bell, 2009; Jandaghian & Akbari, 2018). In London for instance, where the UHI has been extensively studied for summer and winter (Giridharan & Kolokotroni, 2009; Kolokotroni & Giridharan, 2008), the Greater London Authority has highlighted urban albedo as one of the most significant parameters for mitigating the UHI (Greater London Authority, 2006). A review and meta-analysis of 14 studies on the impact of increased urban albedo on ambient air temperatures and heat related mortality found that an albedo rise of 0.1 could reduce the afternoon temperature by 0.10–0.38 °C and the heat related mortality by an average of 1.8% (Santamouris & Fiorito, 2021).

The ability of street canyons to reflect depends on surface reflectance (i.e. surface albedo), which is the reflecting power of a surface in the shortwave region of the electromagnetic spectrum, and on geometry which in the urban context intensifies the radiation absorption by multiple reflections between surfaces. Their significance has received public attention when solar radiation reflected by a newly built skyscraper in London was intense enough to melt parts of a nearby parked car (BBC, 2013). Contrary to flat and unobstructed open surfaces, radiation in urban canyons tends to be intercepted by different surfaces and is subjected to multiple reflections (Qin, 2015) which can result in up to 50 interreflections (Aida & Gotoh, 1982), thus intensifying the radiation absorption between building surfaces (Oke, 1987;

E-mail address: a.g.kotopouleas@kent.ac.uk (A. Kotopouleas).

https://doi.org/10.1016/j.solener.2021.09.074
Received 16 July 2021; Accepted 24 September 2021
Available online 23 October 2021

Fig. 1. (a) The case study area in Islington, London (source: Google Maps), (b) the 1:10 scaled model built with real building materials, (c) accurate model layout setting and (d) pyranometers taking incident and reflected radiation measurements at canyon's eaves level using IR filters and shade.

Table 1
Geometrical figures of model street canyon and material proportionality at its brickwork and paved phase.

		SE-facing façade	Horizontal	NW-facing façade
General	Terrace length (m)	6.85	n/a	7.60
	Height to eaves (m)	0.98	n/a	0.96
	Height to ridge (m)	1.36	n/a	1.26
	Surface area of pitched roof (m^2)	7.79	n/a	6.81
Façades	Total surface area (m^2)	6.71	n/a	7.24
	Surface area with brick (m^2)	4.89	n/a	5.28
	Surface area with glass (m^2)	1.62	n/a	1.74
	Surface area with plywood/doors (m^2)	0.20	n/a	0.22
Street	Total surface area (m^2)	n/a	13.06	n/a
	Surface area with concrete paving (m^2)	n/a	2.3	n/a
	Surface area of tarmac (m^2)	n/a	10.76	n/a

Santamouris & Asimakopoulos, 1997).

Using a three-dimensional canopy model to determine the nocturnal rate of rural and urban environments, (Oke, 1981) highlighted canyon geometry as a critical variable to the magnitude of the UHI. The earliest study to use physical modelling to investigate the influence of surface irregularity were carried out in Japan where scale model arrays were developed using 0.15 m cubic concrete blocks. It was shown that both flat and irregular surfaces present diurnal and seasonal albedo variation, with the irregular surfaces contributing to a 20% lower effective albedo than flat surfaces (Aida, 1982). A follow-up study used the Monte Carlo photon tracking method to develop a numerical two-dimensional canyon model to estimate urban albedo variations due to urban canyon geometry (Aida & Gotoh, 1982). The data from these studies were later used for validation purposes by several other studies which developed numerical models to investigate canyon albedo (Fortuniak, 2008; Sievers & Zdunkowski, 1985) and urban albedo (Kondo et al., 2001). Another study used the Monte Carlo method to develop a meteorological-oriented urban canyon model which took into account the thermal conduction in the canyon's facets (Montávez et al., 2000). An experimental set-up similar to Aida's, comprising 0.15 m cubic concrete blocks regularly distributed on 3.6 × 3.6 m flat concrete plates, was used in the development of a three-dimensional model for regular building arrays (Kanda et al., 2005). Although the study investigated a wider range of surface geometries, the findings were yet limited to a single surface material (concrete).

A common finding between studies on the relationship between street canyon albedo and height-to-width (H/W) ratio (i.e. height of walls to distance between buildings) is the reduction of canyon albedo with increasing building height (Arnfield, 2003; Chimklai et al., 2004; Fortuniak, 2008). Geometry has also been shown to be an important parameter to the diurnal variability of albedo at urban level, where building height heterogeneity has been found to have an increasing effect on albedo (Kondo et al., 2001; Sailor & Fan, 2002; Yang & Li, 2015).

Experimental studies of scale models using real urban forms are rarer in literature. One of the most comprehensive studies on the complexity of the urban texture affecting the amount of light absorbed, investigated a central area of 400 × 400 m from the cities of London, Berlin and Toulouse (Steemers et al., 1998). Using models identical in plan area and scale, constructed of the same materials and all painted subsequently at three different colours, highlighted that the denser urban fabric resulted effectively in the lowest urban albedo at all the surface paint reflectances.

The role of urban fabric is critical in the reduction of solar radiation entrapment in urban canyons. The thermal performance of urban materials is largely determined by their thermal and optical properties with surface reflectance and emissivity to long wave radiation being the most decisive parameters. Surface roughness and moisture impact the rate of sensible and latent heat flux respectively, thus are additional factors to

Fig. 2. Experimental phases of street canyon under investigation with street-level and façade material tests.

Fig. 3. (a) Albedo spot measurements at the real site (b) measurement points and (c) real site vs. physical model spot measurements.

surface reflectance (Sailor & Fan, 2002). An experimental investigation of 93 commonly used paving materials found that tiles with a smooth and flat surface were cooler than tiles with a rough and anaglyph surface, highlighting surface texture (roughness) as an important physical characteristic affecting surface reflectance alongside colour and material type (Doulos et al., 2004). Another study on paving materials identified a diurnal surface albedo pattern, where pavement surface albedo was high in the early morning and late afternoon, and low and constant over time around midday (Li et al., 2013). Focusing on façades, and more specifically on the effect of typical coated (SnO_2) glazed façades on canyon albedo, a simulation study showed that increasing the window to wall ratio has a decreasing effect on canyon albedo. This

Table 2
Descriptive values of incident radiation and canyon albedo before and after the application of concrete paving on the horizontal in June-September.

	N*		Mean	Min.	Max.	Std. Dev.
100% tarmac	4191	Incident radiation (W/m^2)	484	11	1197	286
		Canyon albedo	0.11	0.02	0.16	0.01
82% tarmac & 18% paving	733	Incident radiation (W/m^2)	536	42	982	232
		Canyon albedo	0.12	0.05	0.20	0.02

*N = the count of 5-minute averages.

trend was consistent for all H/W ratios tested and under both direct sunlight and diffuse sky conditions, while the observed albedo reduction was shown to decrease as the sun elevation increased (Tsangrassoulis & Santamouris, 2003).

Increasing surface reflectance has been identified as an effective way of lowering ambient temperatures. A study for Toronto and Montreal, Canada, estimated that an increase of the background albedo from 0.2 to 0.65 for roofs, 0.60 for walls and 0.45 for the ground could lead to 1–2 °C reduction in ambient temperature (Jandaghian & Akbari, 2021). Because of their high solar reflectance and high emissivity, cool materials have been systematically studied in terms of thermal performance and albedo impact (Kolokotroni et al., 2013; Santamouris et al., 2011; Synnefa et al., 2007). A modelling study for Athens, Greece, found that a large-scale increase of rooftops' albedo could lower ambient air temperature by 2 °C (Synnefa et al., 2008). In addition to the traditional cool materials, retroreflective materials have been recently researched as an alternative strategy for UHI mitigation (Rossi et al., 2015; Yuan et al., 2015). Using a scaled model comprising three buildings 250 cm long × 20 cm wide × 60 cm high and two canyons 60 cm wide with bitumen horizontal, a study in Italy demonstrated that retroreflective façade applications resulted in increased canyon albedo (Battista et al., 2021).

Nowadays, designers, planners and urban development professionals use urban albedo values from the literature to inform building energy and thermal simulations. However, the multitude of factors involved in the radiation exchange within canyons and the complexities at the urban level suggest a constant albedo value for a given location may not be accurate enough, particularly for urban settings with substantial surface pluralism. Moreover, despite the wealth of studies on the performance of urban materials, experiments have been predominantly carried out in isolation without considering the urban geometrical complexities, while the few studies involving scale models investigated theoretical buildings and were limited to a single material. Focussed on the impact of urban fabric on street canyon albedo, this paper presents findings from an experimental investigation that used a large physical model of an actual residential area to study the effect of common urban materials on canyon albedo and inform the development of an urban albedo calculator that predicts changes in urban albedo in relation to changes in urban fabric and solar altitude.

2. Methods

2.1. The 1:10 scaled physical model

The study developed a 1:10 scaled physical model of an actual residential area in Islington, London, comprising over 50 terraced houses across three street canyons (Fig. 1a). The case study was chosen through preliminary surveys carried out within the Greater London using 80 locations previously studied for UHI (Kolokotroni & Giridharan, 2008; Watkins et al., 2007). The selected area was extensively surveyed and scanned using a 3D scanning camera to collect detailed data on block sizes, canyon geometry and urban materials which informed the development of the 1:10 scaled physical model (Fig. 1b). The marginal latitude difference between London (51.5074° N) and Canterbury (51.2802° N) enabled the development of the model in the University of

Table 3
Descriptive values of incident radiation and canyon albedo before and after the application of grass on the horizontal in October.

	N*		Mean	Min.	Max	Std. Dev.
82% tarmac & 18% paving	216	Incident radiation (W/m^2)	159	8	404	97
		Canyon albedo	0.09	0.06	0.16	0.02
82% grass & 18% paving	216	Incident radiation (W/m^2)	182	2	483	129
		Canyon albedo	0.16	0.11	0.26	0.02

*N = the count of 5-minute averages.

Table 4
Descriptive values of incident radiation and canyon albedo before and during snow coverage on the horizontal in February.

	N*		Mean	Min.	Max	Std. Dev.
82% tarmac & 18% paving	564	Incident radiation (W/m^2)	101	0	391	102
		Canyon albedo	0.04	0.01	0.5	0.04
100% snow	581	Incident radiation (W/m^2)	94	0.01	523	109
		Canyon albedo	0.43	0.01	0.92	0.16

*N = the count of 5-minute averages.

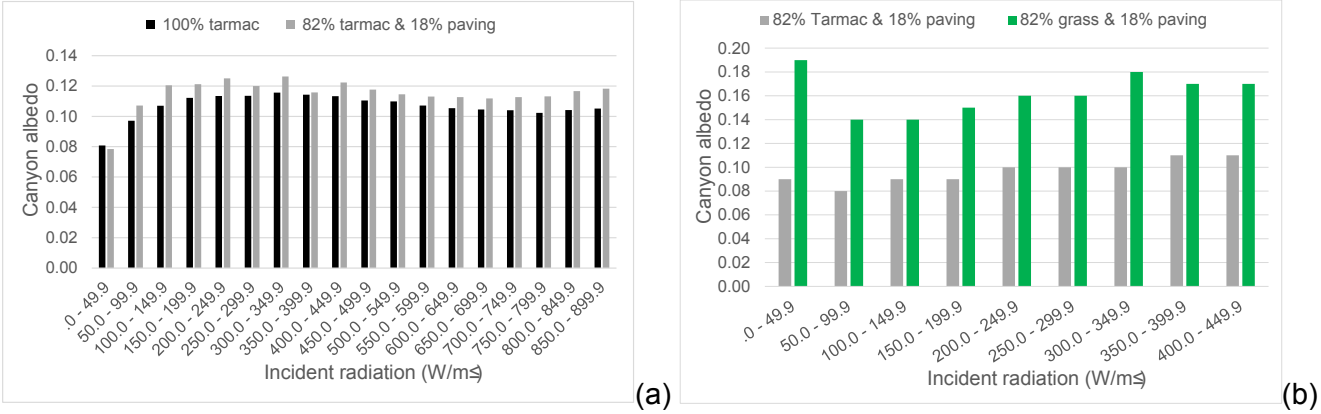

Fig. 4. Effect of concrete paving and grass on canyon albedo.

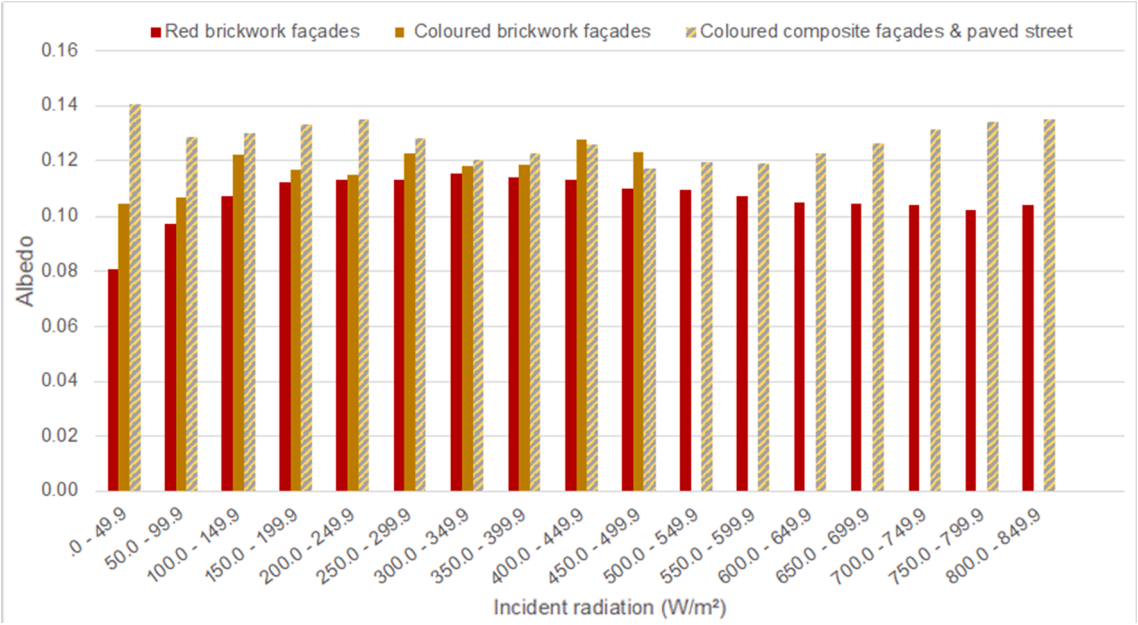

Fig. 5. Change of canyon albedo due to façade colour and combined effect of paving and façade colour.

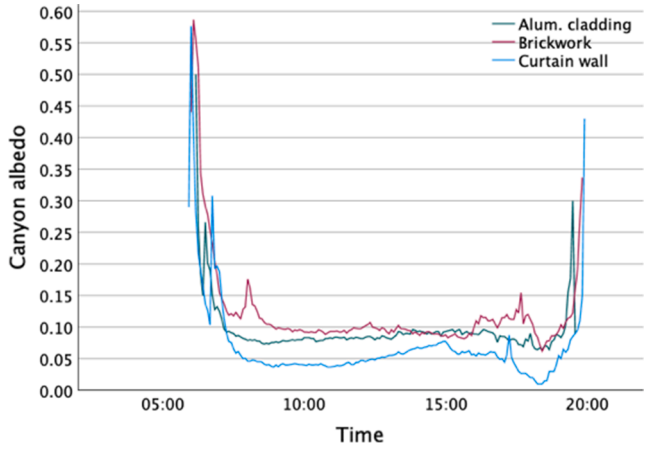

Fig. 6. Average diurnal profile of canyon albedo during the brickwork, aluminium cladding and curtain wall façade applications.

Kent campus, in Canterbury, for logistical efficiency. Since a 50 m radius is considered a suitable area to capture urban climate variations in a London setting (Kolokotroni & Giridharan, 2008), the model was built in a 5 m radius area.

The layout setting was carried out using a theodolite and appropriate setting plan to maintain the correct orientation and street alignments (Fig. 1c). The surrounding trees were trimmed to avoid the blocking of incoming solar radiation while taking into account the nesting periods of birds. The building blocks were made of 9 mm thick plywood cut to size and built on tarmac ground. The façades were developed to accurately reproduce the materials' proportionality on the façades at the real site. Brick, the most common material in London, was used as a module. Bay windows and glazed openings were modelled using the sizing measurements from the field surveys while the size of inaccessible glazing (e.g. at the rear of the properties) was determined from point cloud data collected during the 3D scanning surveys. The original built model comprised approximately 5400 red brick slips, 490 cut-to-size clear float glass pieces 4 mm thick and with a U-value of 5.8 W/m^{2}K and 600 clay roof tiles used for the roofs. Doors were also represented using plywood.

2.2. Radiation measurements from physical model

A monitoring protocol was developed to enable thorough measurements of solar irradiance and reflected radiation at different points within the model. In the middle of the modelled street canyons, a pair of back-to-back pyranometers measured incoming and reflected radiation at eaves level, while measurements of incident irradiance at street level were taken at the two junctions where geometry changes substantially. Another pair of back-to-back pyranometers was suspended in the middle of the model, on a box section at a height of 2.25 m (i.e. 1 m above the tallest building), capturing incident and reflected radiation for the entire model. All pyranometers employed had a spectral range of 285–3000 $\times$ 10^{-9} m. Measurements were taken at 1 s intervals and were recorded in a Campbell Scientific datalogger powered from a battery and a 30 W PV panel.

The measurement protocol underwent successive refinements during the experiment, including the testing of shades and infrared (IR) filters of different shape and size. The application of shades on downward-looking pyranometers (Fig. 1d) was aimed at restricting the view to the area under investigation. The objective of using IR filters was to block the visible component of the electromagnetic spectrum, therefore transmitting infrared, which is primarily responsible for heat transfer, thus enabling the measurement of IR albedo. The dome-shaped IR filters (Fig. 1d) were developed in the University of Kent using a 0.5 mm thick IR filter (acrylic) sheet and had excellent transmittance up to a maximum of approximately 90% in the infrared region from 850 nm to 2000 nm, 50% transmission at 780 nm and effectively 0% below 740 nm in the visible spectrum. The entire model area was encircled by black tarpaulins to block noise radiation from the surrounding environment.

2.3. The street canyon under investigation and its experimental phases

This paper focuses on results from the modelled street canyon that accommodated material changes on both vertical (façades) and horizontal (street-level) surfaces to evaluate their impact on urban canyon albedo. The canyon, NE-SW oriented, included 22 terraced 3-storey building blocks with H/W ratio of 1/1.6 (Table 1).

The experimental phases of the canyon are shown in Fig. 2. In the original build (Fig. 2a), façades comprised 73% red bricks, 24% glass and 3% wood. In its "brickwork" phase (Fig. 2b), bricks were coloured to

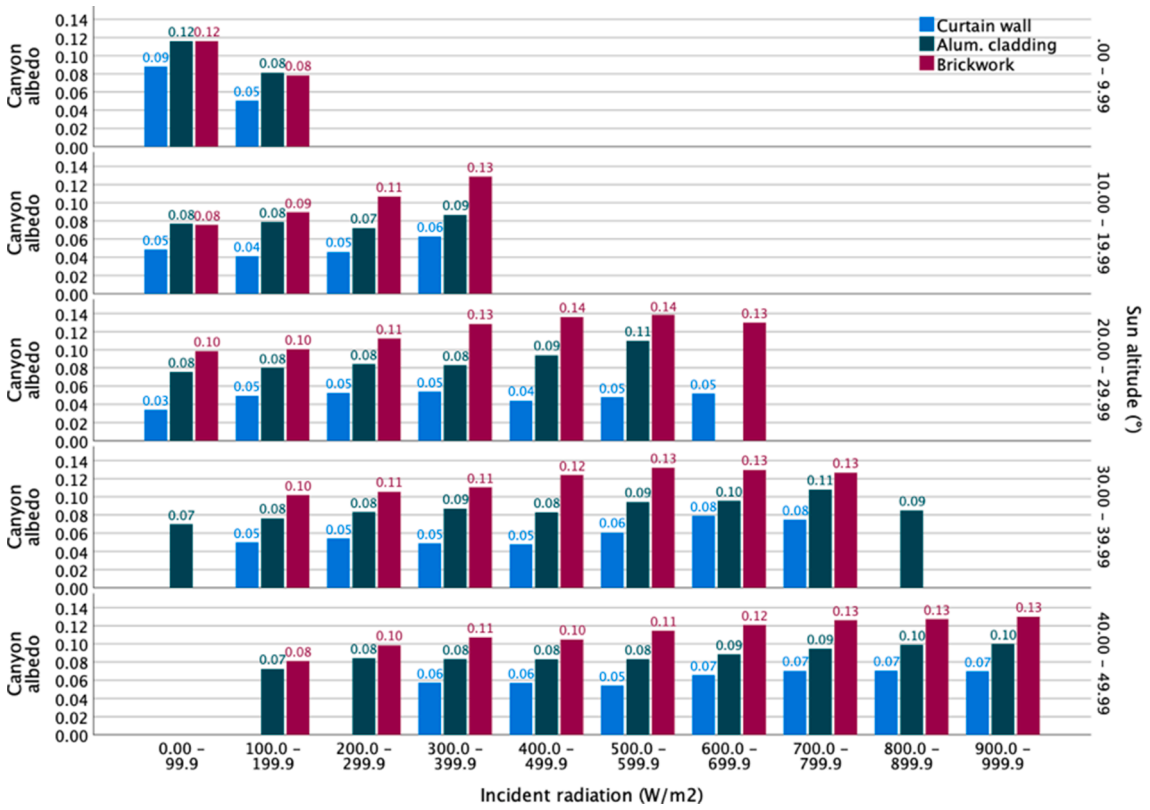

Fig. 7. Variation of average canyon albedo by solar irradiance and sun altitude with brickwork, aluminium cladding and curtain wall façade applications.

resemble the brick colours in the real site with the proportion and distribution of façade materials remaining unchanged. In the "curtain wall" and "aluminium cladding" applications (Fig. 2c-d), for logistical purposes, 3 m^2 of the material under investigation were installed uniformly on either side of the canyon, spanning symmetrically from its middle where the pyranometers were located, covering 40–44% of the façades' surface area. The aluminium cladding was an extruded aluminium weatherboard system powder coated in RAL 7016 and the curtain wall was 4 mm toughened glass (U-value = 5.8 W/m^2K) backed with a black out film. Interventions on the horizontal included the addition of concrete paving (Fig. 2e), the substitution of tarmac with grass (Fig. 2f) and a weather-induced application, snowfall (Fig. 2g).

3. Results

The analysis of data collected from the physical model was carried out using daytime (sunrise to sunset) 5-minute averaged data from dry days (i.e. days with no rainfall during daytime). Data from days with rainfall were used for the assessment of the impact of rainfall on albedo. To enable the investigation of albedo variation between different irradiance levels as a result of the varying street and façade reflectance, the measured spectrum of incident solar radiation was binned into 50 W/m^2 bins.

3.1. Canyon albedo profile at 1:10 scale vs. Full scale

To investigate the horizontal and vertical profile of albedo, spot measurements with a handheld albedometer were taken at successive points across the three street canyons at the real site (Fig. 3a-b). Using a hydraulic platform, the albedo at each point was measured at three different heights: street level (1.2 m), 2nd floor level (4.9 m) and eaves level (9.7 m). Subsequently, on a day with similar sky conditions and in the same hours, another set of spot measurements was taken at the respective points and scaled-down heights within the physical model.

The results (Fig. 3c) revealed a great convergence between the two scales; in the real site the average albedo was 0.08 at street and 2nd floor level and slightly higher, 0.09, at eaves level, while the respective mean values in the physical model were 0.09 throughout. Small deviations were observed at the two junctions where the model resembled partly the surrounding geometrical characteristics. In both scales, the variation of albedo horizontally and vertically was marginal, in the range of 0.01–0.04. Overall, the agreement between the two scales alongside the minimal variation of albedo demonstrated the dominant effect of the horizontal (tarmac) surface on the radiation exchange in both scales.

3.2. Effect of street-level surface materials on canyon albedo

Four different horizontal surfaces were experimentally investigated: the original tarmac ground, combination of tarmac and concrete paving, combination of grass and concrete paving, and snow (Fig. 2a & e-g). The tests took place at different times in the year, therefore the effect of each phase was comparatively assessed against the canyon's albedo right before each change took place to eliminate the impact of material ageing and varying solar angles.

The introduction of paving was among the early interventions aimed at representing the real setting. For this purpose, concrete paving, 0.18 m wide, was added across the modelled street canyon (Fig. 2e) to occupy 18% of the total horizontal surface area in line with the case study setting. The addition of paving increased canyon albedo by 9%, from 0.11 to 0.12 (Table 2), with the magnitude of increase seen almost constant across the measured spectrum of solar irradiance (Fig. 4a).

The substitution of tarmac with grass took place in a different season (autumn), when the model was paved, façades were coloured (Fig. 2f) and the street canyon presented an average albedo of 0.09. The green-dominated horizontal, comprising 82% grass and 18% paving, led to a sharp rise in albedo to 0.16, denoting an increase of the canyon's ability to reflect radiation back to the sky by 70% (Table 3). The increase was observed throughout the measured irradiance range (Fig. 4b) and was

Table 5
Descriptive values of canyon albedo for brickwork, aluminium cladding and curtain wall façade applications.

	N*		Mean	Min.	Max.	St. Dev.
Curtain wall on both façades	2019	No rainfall during daytime	0.06	0.01	0.76	0.05
	633	Rainfall during daytime	0.04	0.01	0.15	0.02
Curtain wallon NW-facing façade	639	No rainfall during daytime	0.08	0.01	0.71	0.06
	314	Rainfall during daytime	0.07	0.01	0.63	0.09
Curtain wallon SE-facing façade	224	No rainfall during daytime	0.04	0.01	0.23	0.02
	780	Rainfall during daytime	0.04	0.01	0.50	0.04
Alum. cladding on both façades	1513	No rainfall during daytime	0.09	0.01	0.54	0.04
	162	Rainfall during daytime	0.07	0.03	0.24	0.04
Alum. Cladding on NW-facing façade	420	No rainfall during daytime	0.10	0.01	0.39	0.03
	1275	Rainfall during daytime	0.09	0.01	0.63	0.05
Alum. cladding on SE-facing façade	822	No rainfall during daytime	0.10	0.02	0.46	0.04
	148	Rainfall during daytime	0.08	0.02	0.20	0.02
Brickwork on both façades	2390	No rainfall during daytime	0.11	0.01	0.69	0.06
	1028	Rainfall during daytime	0.07	0.01	0.53	0.05

*N = the count of 5-minute averages.

highest for low solar irradiance levels (<50 W/m^2) corresponding to low sun altitude (5–10°).

Snowfall occurred at a time when the canyon's SE- and NW-facing façades were curtain wall and brickwork respectively demonstrating a mean albedo of 0.04. The effect of the entirely white horizontal was an elevenfold increase of canyon albedo to a mean value of 0.43, representing an increase of nearly 1000% (Table 4).

The measurements taken in different seasons while the horizontal surface was paved revealed significant variations in canyon albedo. More specifically, with the horizontal being 82% tarmac and 18% paving, canyon albedo was 0.12 in summer, 0.09 in autumn and 0.04 in winter (Tables 2-4). Some of the variation could be attributed to the differentiation in façades. However, when only dry days were considered, the magnitude of albedo change between the different seasons highlighted the effect of seasonality.

3.3. Effect of vertical surfaces on canyon albedo

3.3.1. Façade colour

Following the application of paving, façades were coloured with masonry paint using hues similar to those on site, determined by means of a colour sensing scanner. Representing the physical model façade colour in line with actual site was found to have a similar effect to that of paving, raising canyon albedo by 10% from 0.11 to 0.12. It was, however, the combined effect of façade colour and paving that demonstrated the highest impact, leading to an average albedo increase of 20%, to 0.13 (Fig. 5).

3.4. Impact of façade materials

The application of brickwork, aluminium cladding and curtain wall façades enabled the comparative analysis of three façade types commonly used in urban areas. Throughout the tests involving façade material changes, the ground was in the 82% tarmac and 18% paving status.

With all three façade types the canyon's diurnal albedo presented a U-shaped profile, where albedo increases rapidly during sunrise, lowers soon after and presents little variation during the daytime, and peaks again just before the sunset (Fig. 6). The observed pattern was the combined result of the canyon's orientation, façade material and alteration of sun altitude. Material specularity starts having an effect in the morning peak due to the very low sun angle, when the radiation beam strikes first the SE-facing façade and a fraction of it is reflected to the opposite façade, street and sky. As the sun angle increases, the shade on the street recedes and the effect of the horizontal surfaces increases; the street starts to receive beam radiation and because of its considerably lower reflective power it contributes to lower canyon albedo which then varies less throughout the daytime until the evening peak (also due to low sun angle).

The results also showed that, controlling for sun altitude range, canyon albedo increases with irradiance highlighting its variability under different sky conditions. For sun angles between 40 and 49.9° for instance, a midday sun altitude range for April, canyon albedo with brickwork façades would rise from 0.08 for irradiance 100–199.9 W/m^2 (cloudy sky) to 0.13 for irradiance over 800 W/m^2 (clear sky) (Fig. 7). The respective change in albedo for aluminium cladding façades would be from 0.07 to 0.10. The magnitude of increase with irradiance was highest with brickwork façades and least with curtain wall because of the high transmission of glass.

The results were also indicative of the influence of solar angle on the radiation exchange within the canyon. For example, for radiation in the range of 500–599.9 W/m^2 and the sun at 20–29.9° the canyon had an albedo of 0.14 with brickwork and 0.11 with aluminium cladding façades (Fig. 7). For the same radiation but higher sun altitude at 30–39.9° albedo dropped to 0.13 and 0.09, and was further reduced to 0.11 and 0.08 respectively for 40–49.9°, highlighting the prevalent role of façades at low sun angles and of the horizontal surface at high sun angles in the particular canyon orientation.

Aluminium cladding and brickwork façades were seen to contribute to higher reflectance from the canyon under all sky conditions, across the measured irradiance and sun altitude ranges (Fig. 7), resulting in an average canyon albedo of 0.09 and 0.11 respectively. In contrast, curtain wall façades plunged the canyon's albedo to an average of 0.06 (Table 5). The maximum difference observed in certain irradiance and sun altitude ranges between curtain wall and aluminium cladding

Table 6
Measured surface albedo and surface IR albedo of materials used in the physical model.

	White bricks	Magnolia bricks	Buff lime bricks	Red bricks	Concrete paving	Glass	Alum. cladding	Roof tiles	Plywood	Tarmac
Albedo	0.73	0.65	0.42	0.31	0.27	0.06	0.22	0.21	0.40	0.12
Infrared albedo	0.72	0.67	0.62	0.42	0.29	0.04	0.28	0.30	0.53	0.15

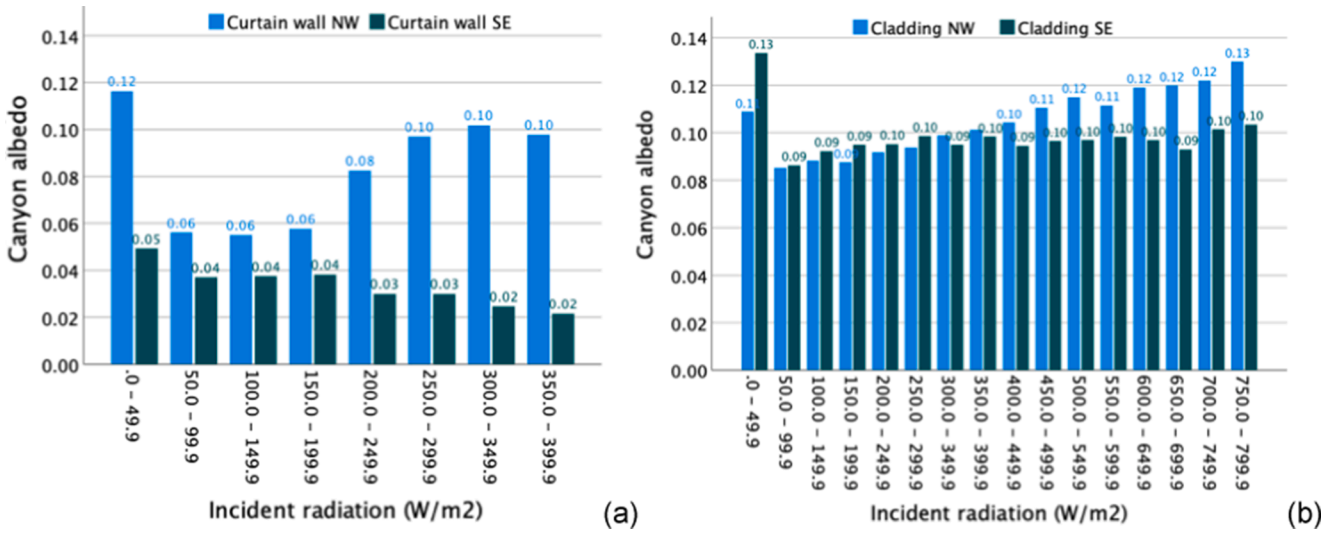

Fig. 8. Canyon albedo by irradiance during the SE- and NW-facing façade applications of (a) curtain wall and (b) aluminium cladding.

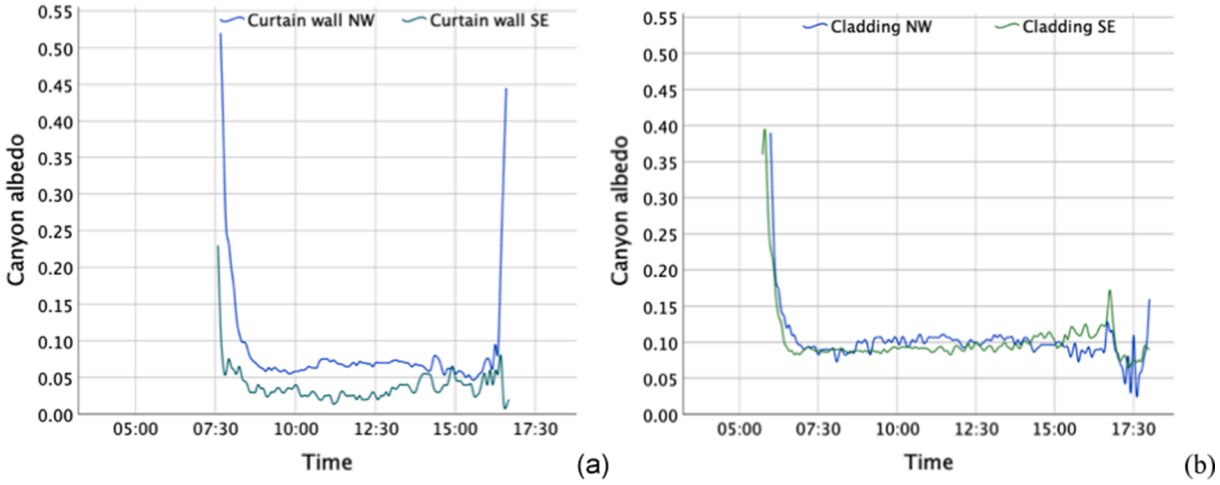

Fig. 9. Diurnal canyon albedo profile during the SE- and NW-facing façade applications of (a) curtain wall and (b) aluminium cladding.

façades was 0.05 while the highest difference between curtain wall and brickwork façades was 0.09 (Fig. 7).

3.5. The influence of orientation

To investigate the effect of orientation on canyon albedo, measurements were also taken with the curtain wall and aluminium cladding applied only on one side of the canyon at a time while keeping the opposite façade as brickwork.

The application of curtain wall on the NW-facing façade resulted in an average canyon albedo of 0.08, whereas the curtain wall on the SE-facing façade led to a 50% reduction leading to an average canyon albedo of 0.04 (Table 5). This is because the sunlight striking first the SE-facing façade - the part of the canyon receiving direct sunlight for most of daytime - was largely transmitted due to the particularly low surface albedo of glass (Table 6), therefore eliminating interreflections within the canyon. The difference between the two applications increased with irradiance (Fig. 8a) as a result of the greater increase of brickwork's reflectance at higher irradiation levels, thus having higher values at midday (Fig. 9a). There was also considerable differentiation observed in the morning and late afternoon peaks due to the low angle of incidence.

On the other hand, the respective SE and NW-facing façade applications of aluminium cladding showed only a marginal differentiation at irradiance levels over 400 W/m^2 (Fig. 8b) and a similar diurnal albedo profile (Fig. 9b), indicating that the influence of orientation on canyon albedo is a combined effect of geometry and material type. However, much depends on the surface reflectance of the façade material where sunlight strikes first.

3.6. Effect of rainfall

The various experimental phases saw significant weather-induced variations in albedo, particularly between dry and rainy conditions. The mean daily canyon albedo was correlated with the daily (24 hrs) amount of rainfall ($r = -0.25$; $p < 0.01$), with the direction of the correlation indicating a lower albedo with a higher level of rainfall.

In its original build phase, the canyon's average albedo was 0.11 on dry days and 0.08 on rainy days, representing a 27% reduction. Moreover, the observed rise of albedo because of the addition of concrete paving and façade colour was seen to vanish on rainy days: canyon albedo was 33% lower in its paved-only phase (from 0.12 to 0.08) and 20% lower when it was paved and coloured (from 0.13 to 0.11) (Nikolopoulou et al., 2020).

Reductions of similar magnitude were also observed during the façade material tests. The rain-induced reduction of canyon albedo was

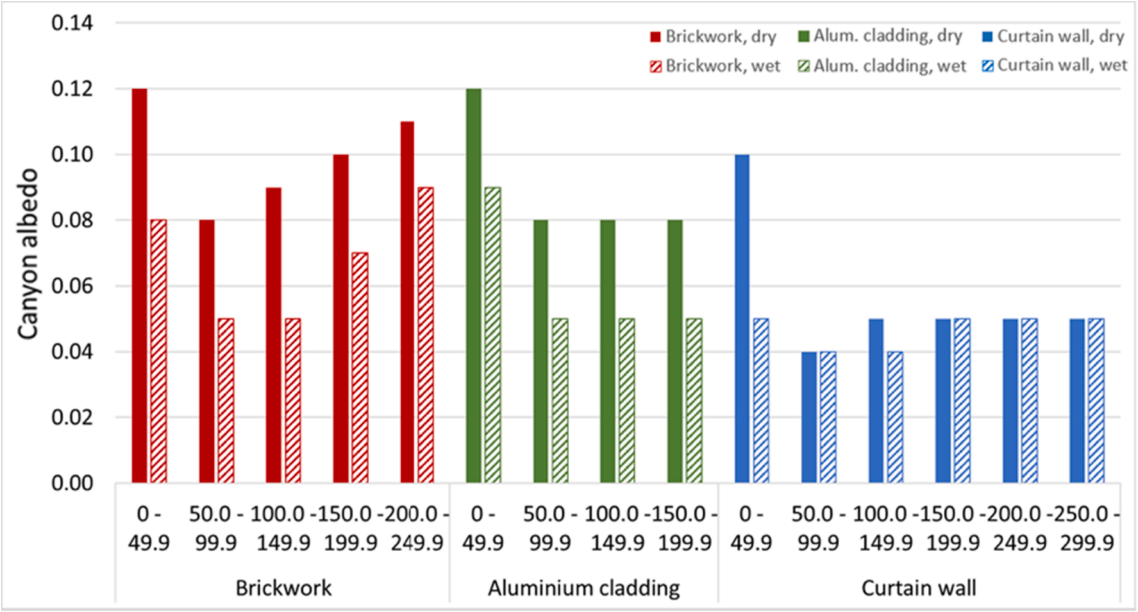

Fig. 10. Canyon albedo variation across measured irradiance range in dry (no rainfall during daytime) and wet (rainfall during daytime) conditions during the different façade material applications.

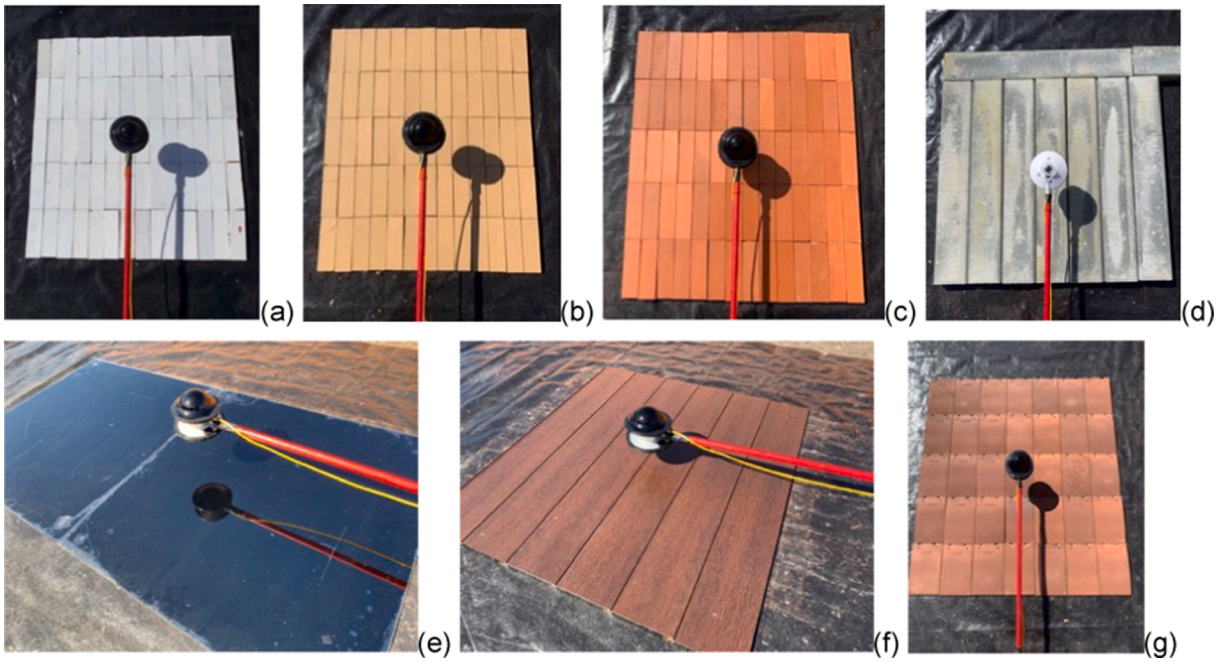

Fig. 11. Spot measurements of surface reflectance and surface infrared reflectance of materials used in the physical model (a) white bricks, (b) buff lime bricks, (c) red bricks, (d) concrete paving, (e) glass, (f) aluminium cladding and (g) clay roof tiles. (For interpretation of the references to colour in this figure legend, the reader is referred to the web version of this article.)

36%, 33% and 22% for brickwork, curtain wall and aluminium cladding applications respectively (Fig. 10). While the percentage reduction was of a similar order, the absolute reduction of canyon albedo while in aluminium cladding (0.02) and curtain wall (0.02) was half the reduction with brickwork façades (0.04), highlighting the role of material permeability and surface roughness, where water slips off the non-porous glass and aluminium panels, restoring their (dry) albedo quicker than brick.

3.7. Infrared albedo

Spot measurements were undertaken using a handheld albedometer to measure the surface reflectance and IR reflectance of the materials used in the physical model (Fig. 11). All material samples were new (not aged) at the time of measurements, except for the tarmac ground.

The reflectance of coloured bricks was found to vary from 0.31 for red bricks to 0.73 for white bricks indicating the dominant influence of surface colour on reflectance over the material type itself (Table 6). The aluminium cladding had lower surface reflectance than brickwork while the glass used in the curtain wall application demonstrated the lowest

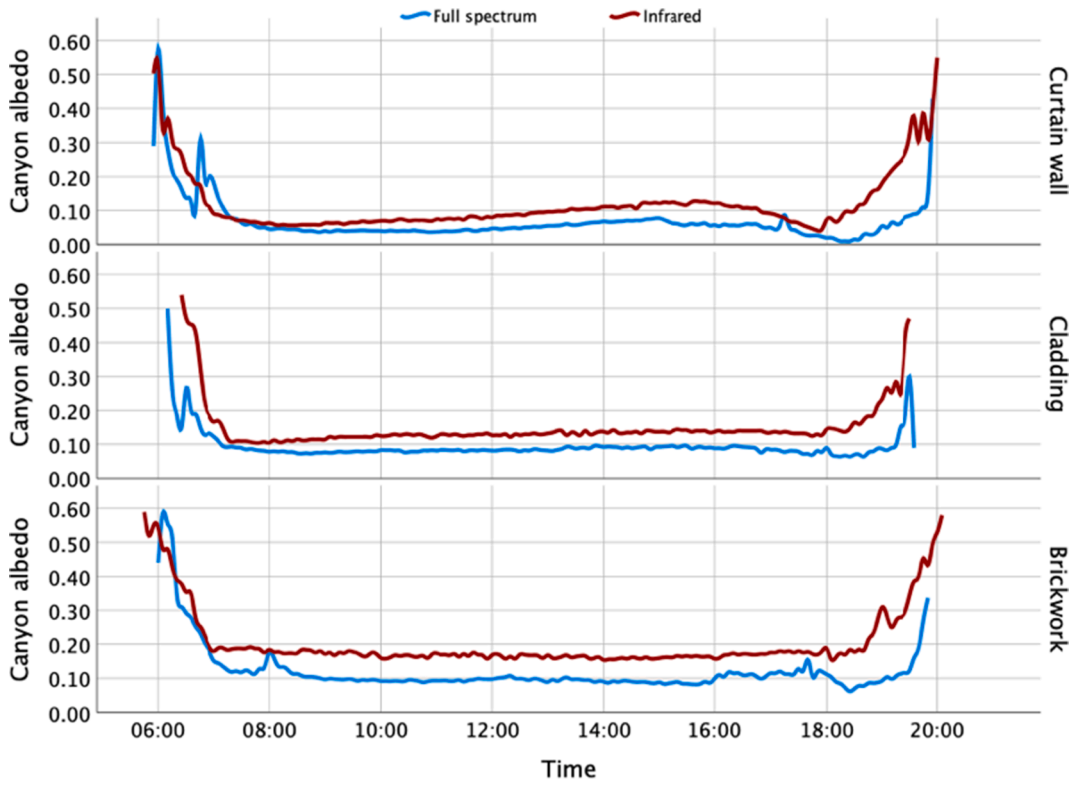

Fig. 12. Average diurnal profile of full spectrum and infrared canyon albedo for brickwork, aluminium cladding and curtain wall façade applications.

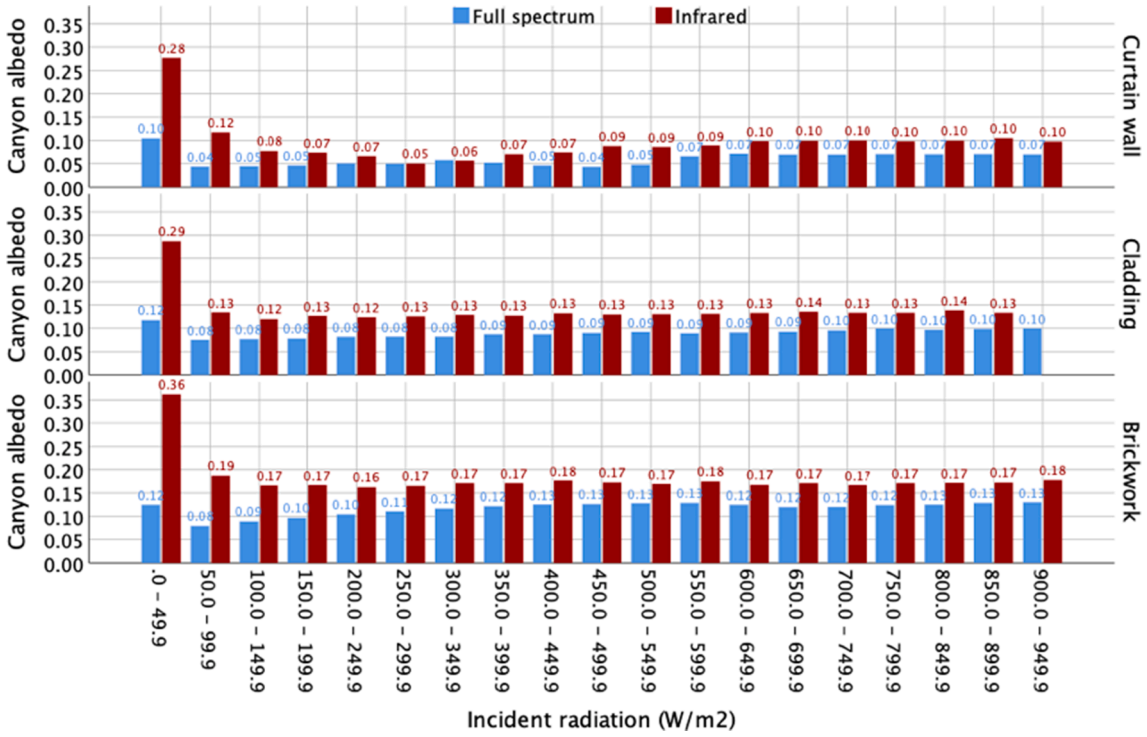

Fig. 13. Comparison of average infrared and full spectrum canyon albedo with curtain wall, aluminium cladding and brickwork façades across the measured irradiance spectrum.

reflectance (0.06). In the infrared, brighter surfaces had higher reflectance as expected, with the lowest values demonstrated by tarmac (0.15) and glass (0.04).

The three façade types were also tested in terms of their contribution to the canyon's reflective power in the infrared. The diurnal profile of IR albedo followed the U-shaped pattern of full spectrum albedo with peaks in early morning and late evening and an almost flat trend during the daytime (Fig. 12).

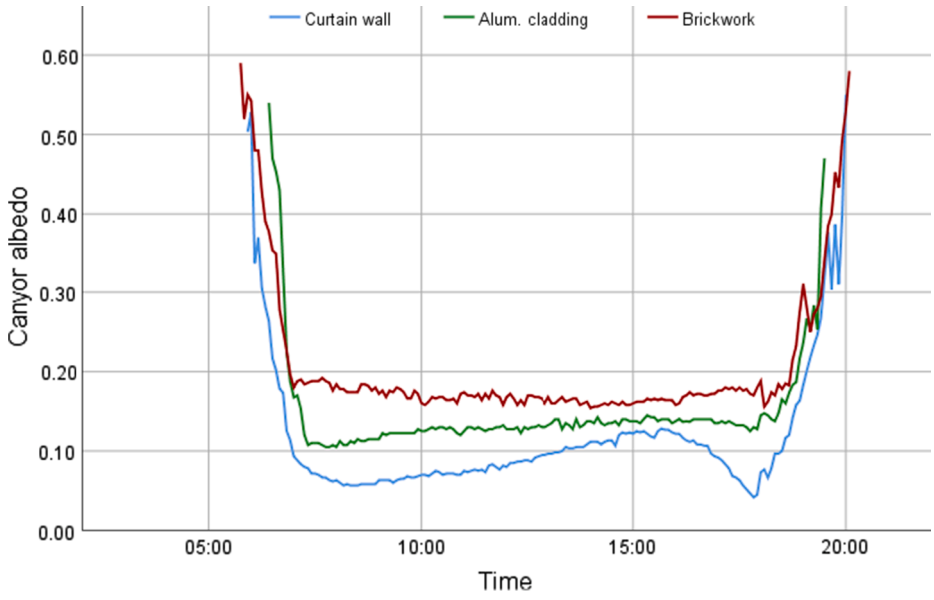

Fig. 14. Average diurnal variation of canyon infrared albedo with curtain wall, aluminium cladding and brickwork façades.

In all three applications, the canyon's albedo in the infrared was higher with the average difference between IR and full spectrum albedo being 0.04, 0.05 and 0.06 for curtain wall, aluminium cladding and brickwork façades respectively, and having the highest values at low irradiance (<50 W/m^2) corresponding to the lowest sun altitudes (<5°) (Fig. 13).

The canyon's ability to reflect infrared radiation was significantly higher throughout the daytime with the aluminium cladding and brickwork façade applications (Fig. 14), which contributed to an average canyon IR albedo of 0.14 and 0.20 respectively (up by 56% and 82% compared to full spectrum canyon albedo) whereas the canyon IR albedo with the curtain wall was 0.11.

4. Discussion

The investigation of the effect of urban fabric using a 1:10 scale physical model showed that both horizontal and vertical surfaces can drive significant changes to the radiation exchange within urban canyons. The introduction of concrete paving occupying nearly a fifth of the horizontal tarmac area was found to increase canyon albedo by 9% (Fig. 4a) while the particularly high increases observed due to the grass (from 0.09 to 0.16; Table 3) and snow applications on the horizontal surface (from 0.04 to 0.43; Table 4) are indicative of the magnitude of albedo change that extensive changes at street-level can bring.

The testing of brickwork, aluminium cladding and curtain wall façade applications demonstrated the effect of commonly used façade materials on the ability of urban canyons to reflect radiation. Curtain wall was found to be contributing to considerably lower canyon albedo (0.06; Table 5), in agreement with the simulation study by (Tsangrassoulis & Santamouris, 2003) where increasing the façade surface area covered by glass was shown to have a decreasing impact on canyon albedo. In contrast, aluminium cladding and brickwork façades were seen to be consistently associated with higher canyon albedo values during the day (Fig. 6) and across the measured irradiance range (Fig. 7) resulting in an average canyon albedo of 0.09 and 0.11 respectively (Table 5). The investigation of albedo in the infrared revealed that brickwork façades resulted in 43% and 82% higher canyon albedo than curtain wall and aluminium cladding façades respectively (Fig. 14), in agreement with the measured surface reflectance of the individual materials (Table 6), thus making curtain wall systems less preferable applications in terms of avoiding thermal energy trapped within street canyons.

The results also revealed the highly dynamic and complex nature of canyon albedo. The diurnal pattern - very similar between the various experimental phases during both full spectrum and IR albedo measurements (Fig. 12) - was characteristic for the early morning and late evening peaks and the almost constant trend during the daytime. The observed U-shape profile was the combined effect of orientation and sun altitude which alternate the contribution between the horizontal and vertical surfaces to the canyon's reflective power during the day. Controlling for solar altitude, the results showed that the same radiation intensity at different angles contributes to varying canyon albedo values, associating lower sun angles with higher albedo (Fig. 7). Similar measured and predicted diurnal albedo trends have been reported for canyon albedo (Battista et al., 2021; Qin, 2015) and urban albedo (Yang & Li, 2015) confirming the angular dependence of both while emphasising the effect of latitude, canyon H/W ratio and orientation which are the factors largely responsible for the differentiations (e.g. a shallow vs. a deep U-shaped trend) seen in the diurnal profiles between the different studies.

The considerable difference (50%) in canyon albedo observed between the SE- and NW-facing curtain wall applications (Table 5, Fig. 8a & Fig. 9a) further stressed the influence of orientation and highlighted the importance of the reflectance of the surface struck first by direct sunlight. On the other hand, the respective aluminium cladding applications showed no significant differentiation (Table 5, Fig. 8b & Fig. 9b) thus indicating that the effect of orientation depends largely on façade surface reflectance. A comparison to the findings from (Steemers et al., 1998), where the effect of orientation was estimated for Berlin (7%), London (8%) and Toulouse (17%) case studies, shows that orientation can have a varying effect which seems to be more striking at canyon level and fading at city-scale due to other parameters' overtaking effect (e.g. roofs).

The results were also indicative of the influence of sky conditions and rainfall on the dynamic nature of albedo. The upward trend of canyon albedo with increasing irradiance (Fig. 7) underlined the albedo change induced by different cloud cover conditions, where the canyon had a lower reflective ability on overcast and cloudy days when diffuse radiation prevailed, than on clear sky days. Rainfall was seen to reduce the surface reflectance of both horizontal and vertical surfaces, resulting in considerable reductions in canyon albedo between 22% and 36% (Table 5 & Fig. 10). Moreover, the rainfall-induced reduction of canyon albedo during the aluminium cladding and curtain wall applications was half that for brickwork, indicating that façade materials of lower surface

roughness and permeability recover more quickly the reflectance capacity they present in dry conditions. This was particularly noticeable for the curtain wall application, where the albedo reduction due to rain was observed predominantly at very low irradiance levels (Fig. 10).

5. Conclusions

This work developed a 1:10 scaled physical model of a real residential area in London to investigate experimentally the impact of urban fabric on canyon albedo. Different material applications were tested at street level and building façade level while the canyon's reflective power was also assessed in the infrared range and in wet conditions.

Concrete paving was seen to lead to 9% rise in canyon albedo while the substitution of tarmac with grass led to 70% increase indicating the large potential for vegetation to lower the energy absorbed in street canyons. The façade material tests demonstrated that curtain wall contributes to significantly lower canyon albedo throughout the day compared to aluminium cladding and brickwork façades, including in the infrared range, highlighting therefore that curtain wall systems are less favourable for strategies aiming to mitigate the UHI.

The results also demonstrated the varying nature of canyon albedo with irradiance, sun altitude and orientation as well as the high impact of rainfall on the ability of surfaces to reflect which was seen to reduce albedo up to 36%. With canyon albedo varying significantly between different sky conditions as well as between dry and wet conditions, variable albedo values which take into account seasonality and rainfall for a given location would be more appropriate for simulations instead of a fixed all-year-round albedo value. Highlighting the dynamic and complex nature of the radiation exchange within urban canyons these findings pave the way to develop more meaningful and measurable urban design and planning guidelines.

Declaration of Competing Interest

The authors declare that they have no known competing financial interests or personal relationships that could have appeared to influence the work reported in this paper.

Acknowledgements

This project was funded by the UK Engineering and Physical Sciences Research Council (EPSRC) contract no. EP/P025145/1. We are grateful to IBSTOCK Bricks Plc and Marley Ltd Roof specialists for donating the bricks and roof tiles used in the model, and the University of Kent Estates for granting the area where the physical model was built. The authors are also grateful to project partners Prof Maria Kolokotroni and Dr Agnese Salvati, from Brunel University, for organising the hydraulic platform for the albedo measurements at the case study site, and the workshop staff at the University of Kent - particularly Kevin Smith for his invaluable help in the development of the model building blocks, shades and infrared filters and Julien Soosaipillai for his contribution to 3D scanning and point cloud data synthesis.

References

Aida, M., 1982. Urban albedo as a function of the urban structure ? A model experiment. Bound.-Layer Meteorol. 23 (4) https://doi.org/10.1007/BF00116269.

Aida, M., Gotoh, K., 1982. Urban albedo as a function of the urban structure ? A two-dimensional numerical simulation. Bound.-Layer Meteorol. 23 (4) https://doi.org/10.1007/BF00116270.

Anderson, B.G., Bell, M.L., 2009. Weather-related mortality: how heat, cold, and heat waves affect mortality in the United States. Epidemiology 20 (2). https://doi.org/10.1097/EDE.0b013e318190ee08.

Arnfield, A.J., 2003. Two decades of urban climate research: a review of turbulence, exchanges of energy and water, and the urban heat island. Int. J. Climatol. 23 (1) https://doi.org/10.1002/joc.859.

Battista, G., de Lieto Vollaro, E., Grignaffini, S., Ocłoń, P., Vallati, A., 2021. Experimental investigation about the adoption of high reflectance materials on the envelope cladding on a scaled street canyon. Energy 230. https://doi.org/10.1016/j.energy.2021.120801.

BBC (2013, September 2). Walkie-Talkie skyscraper melts Jaguar car parts. https://www.bbc.co.uk/news/av/uk-england-london-23941325.

Chimklai, P., Hagishima, A., Tanimoto, J., 2004. A computer system to support Albedo Calculation in urban areas. Build. Environ. 39 (10) https://doi.org/10.1016/j.buildenv.2004.02.006.

Doulos, L., Santamouris, M., Livada, I., 2004. Passive cooling of outdoor urban spaces. The role of materials. Solar Energy 77 (2), 231–249. https://doi.org/10.1016/j.solener.2004.04.005.

Fortuniak, K., 2008. Numerical estimation of the effective albedo of an urban canyon. Theor. Appl. Climatol. 91 (1–4) https://doi.org/10.1007/s00704-007-0312-6.

Giridharan, R., Kolokotroni, M., 2009. Urban heat island characteristics in London during winter. Sol. Energy 83 (9), 1668–1682. https://doi.org/10.1016/j.solener.2009.06.007.

Greater London Authority. (2006). London Urban Heat Island (LUHI): A Summary for Decision Makers.

Hajat, S., O'Connor, M., Kosatsky, T., 2010. Health effects of hot weather: from awareness of risk factors to effective health protection. The Lancet 375 (9717). https://doi.org/10.1016/S0140-6736(09)61711-6.

Hassid, S., Santamouris, M., Papanikolaou, N., Linardi, A., Klitsikas, N., Georgakis, C., Assimakopoulos, D.N., 2000. The effect of the Athens heat island on air conditioning load. Energy Build. 32 (2) https://doi.org/10.1016/S0378-7788(99)00045-6.

Jandaghian, Z., Akbari, H., 2018. The effects of increasing surface reflectivity on heat-related mortality in Greater Montreal Area, Canada. Urban Climate 25. https://doi.org/10.1016/j.uclim.2018.06.002.

Jandaghian, Z., Akbari, H., 2021. Increasing urban albedo to reduce heat-related mortality in Toronto and Montreal, Canada. Energy Build. 237 https://doi.org/10.1016/j.enbuild.2020.110697.

Kanda, M., Kawai, T., Nakagawa, K., 2005. A Simple Theoretical Radiation Scheme for Regular Building Arrays. Bound.-Layer Meteorol. 114 (1) https://doi.org/10.1007/s10546-004-8662-4.

Kolokotroni, M., Giridharan, R., 2008. Urban heat island intensity in London: An investigation of the impact of physical characteristics on changes in outdoor air temperature during summer. Sol. Energy 82 (11). https://doi.org/10.1016/j.solener.2008.05.004.

Kolokotroni, M., Gowreesunker, B.L., Giridharan, R., 2013. Cool roof technology in London: An experimental and modelling study. Energy Build. 67 https://doi.org/10.1016/j.enbuild.2011.07.011.

Kolokotroni, M., Zhang, Y., Watkins, R., 2007. The London Heat Island and building cooling design. Sol. Energy 81 (1). https://doi.org/10.1016/j.solener.2006.06.005.

Kondo, A., Ueno, M., Kaga, A., Yamaguchi, K., 2001. The Influence Of Urban Canopy Configuration On Urban Albedo. Bound.-Layer Meteorol. 100 (2) https://doi.org/10.1023/A:1019243326464.

Li, H., Harvey, J., Kendall, A., 2013. Field measurement of albedo for different land cover materials and effects on thermal performance. Build. Environ. 59, 536–546. https://doi.org/10.1016/j.buildenv.2012.10.014.

Mishra, A.K., Ramgopal, M., 2013. Field studies on human thermal comfort — An overview. Build. Environ. 64 https://doi.org/10.1016/j.buildenv.2013.02.015.

Montávez, J.P., Jiménez, J.I., Sarsa, A., 2000. A Monte Carlo Model Of The Nocturnal Surface Temperatures In Urban Canyons. Bound.-Layer Meteorol. 96 (3) https://doi.org/10.1023/A:1002600523841.

Nikolopoulou, M., Kotopouleas, A., Giridharan, R., Watkins, R., 2020. Developing an Urban Albedo Calculator for London: the experimental campaign supporting the development of tool. In: CIBSE ASHRAE Technical Symposium.

Oke, T.R., 1981. Canyon geometry and the nocturnal urban heat island: Comparison of scale model and field observations. J. Climatol. 1 (3) https://doi.org/10.1002/joc.3370010304.

Oke, T.R., 1987. Boundary Layer Climates, 2nd ed. Routledge.

Oke, T.R., 1988. Street design and urban canopy layer climate. Energy Build. 11 (1–3) https://doi.org/10.1016/0378-7788(88)90026-6.

Pantavou, K., Theoharatos, G., Mavrakis, A., Santamouris, M., 2011. Evaluating thermal comfort conditions and health responses during an extremely hot summer in Athens. Build. Environ. 46 (2) https://doi.org/10.1016/j.buildenv.2010.07.026.

Qin, Y., 2015. Urban canyon albedo and its implication on the use of reflective cool pavements. Energy Build. 96, 86–94. https://doi.org/10.1016/j.enbuild.2015.03.005.

Rossi, F., Castellani, B., Presciutti, A., Morini, E., Filipponi, M., Nicolini, A., Santamouris, M., 2015. Retroreflective façades for urban heat island mitigation: Experimental investigation and energy evaluations. Appl. Energy 145. https://doi.org/10.1016/j.apenergy.2015.01.129.

Sailor, D.J., Fan, H., 2002. Modeling the diurnal variability of effective albedo for cities. Atmos. Environ. 36 (4) https://doi.org/10.1016/S1352-2310(01)00452-6.

Santamouris, M., Asimakopoulos, D., 1997. Passive Cooling of Buildings. James and James Science Publishers.

Santamouris, M., Fiorito, F., 2021. On the impact of modified urban albedo on ambient temperature and heat related mortality. Sol. Energy 216, 493–507. https://doi.org/10.1016/j.solener.2021.01.031.

Santamouris, M., Synnefa, A., Karlessi, T., 2011. Using advanced cool materials in the urban built environment to mitigate heat islands and improve thermal comfort conditions. Sol. Energy 85 (12). https://doi.org/10.1016/j.solener.2010.12.023.

Sievers, U., Zdunkowski, W., 1985. A numerical simulation scheme for the albedo of city street canyons. Bound.-Layer Meteorol. 33 (3) https://doi.org/10.1007/BF00052058.

Steemers, K., Baker, N., Crowther, D., Dubiel, J., Nikolopoulou, M., 1998. Radiation absorption and urban texture. Build. Res. Inform. 26 (2) https://doi.org/10.1080/096132198370029.

Synnefa, A., Dandou, A., Santamouris, M., Tombrou, M., Soulakellis, N., 2008. On the use of cool materials as a heat island mitigation strategy. J. Appl. Meteorol. Climatol. 47 (11), 2846–2856. https://doi.org/10.1175/2008JAMC1830.1.

Synnefa, A., Santamouris, M., Apostolakis, K., 2007. On the development, optical properties and thermal performance of cool colored coatings for the urban environment. Sol. Energy 81 (4). https://doi.org/10.1016/j.solener.2006.08.005.

Tsangrassoulis, A., Santamouris, M., 2003. Numerical estimation of street canyon albedo consisting of vertical coated glazed facades. Energy Build. 35 (5) https://doi.org/10.1016/S0378-7788(02)00157-3.

Watkins, R., Palmer, J., Kolokotroni, M., 2007. Increased Temperature and Intensification of the Urban Heat Island: Implications for Human Comfort and Urban Design. Built Environ. (1978-), 33(1), 85–96. http://www.jstor.org/stable/23289474.

Yang, X., Li, Y., 2015. The impact of building density and building height heterogeneity on average urban albedo and street surface temperature. Build. Environ. 90, 146–156. https://doi.org/10.1016/j.buildenv.2015.03.037.

Yuan, J., Farnham, C., Emura, K., 2015. Development of a retro-reflective material as building coating and evaluation on albedo of urban canyons and building heat loads. Energy Build. 103 https://doi.org/10.1016/j.enbuild.2015.06.055.